Optimized virtual orbital subspace for faster GW calculations in localized basis

Fabien Bruneval

Citation: The Journal of Chemical Physics **145**, 234110 (2016);
View online: https://doi.org/10.1063/1.4972003
View Table of Contents: http://aip.scitation.org/toc/jcp/145/23
Published by the American Institute of Physics

Optimized virtual orbital subspace for faster *GW* calculations in localized basis

Fabien Bruneval
CEA, DEN, Service de Recherches de Métallurgie Physique, Université Paris-Saclay, F-91191 Gif-sur-Yvette, France

(Received 4 October 2016; accepted 28 November 2016; published online 20 December 2016)

The popularity of the *GW* approximation to the self-energy to access the quasiparticle energies of molecules is constantly increasing. As the other methods addressing the electronic correlation, the *GW* self-energy unfortunately shows a very slow convergence with respect to the basis complexity, which precludes the calculation of accurate quasiparticle energies for large molecules. Here we propose a method to mitigate this issue that relies on two steps: (i) the definition of a reduced virtual orbital subspace, thanks to a much smaller basis set; (ii) the account of the remainder through the simpler one-ring approximation to the self-energy. We assess the quality of the corrected quasiparticle energies for simple molecules, and finally we show an application to large graphene chunks to demonstrate the numerical efficiency of the scheme. *Published by AIP Publishing.* [http://dx.doi.org/10.1063/1.4972003]

I. INTRODUCTION

Many-body perturbation theory[1,2] allows one to calculate the electronic quasiparticle energies, which are physical observables and thus can be compared to photoemission and inverse photoemission experiments. This approach is the method of choice to obtain the electronic states that cannot be obtained through a difference of total energies. Indeed, the so-called ΔSCF procedure only grants access to the highest-occupied molecular orbital (HOMO) and lowest-unoccupied molecular orbital (LUMO) energies.

Within many-body perturbation theory, the famous *GW* approximation to the self-energy has proven very accurate to predict the band structures of extended systems.[3–6] Today, the application of the *GW* approximation to finite systems is becoming more and more frequent and attractive.[7–22]

However, the first systematic convergence study using localized orbitals[12,14] showed the difficulty to obtain absolutely converged *GW* quasiparticle energies. Such a slow convergence rate is not unusual among the correlated methods of quantum chemistry. It has been well-known for years that the Møller-Plesset perturbation theory[23] or coupled-cluster[24] approaches, for instance, experience a slow convergence rate.

Several strategies have been used in the past to obtain converged results within the *GW* approximation or within the correlated methods of quantum chemistry. These approaches comprise the brute force convergence with increasingly large basis sets,[25,26] the fitting of an extrapolation formula,[27–30] an approximation of the remainder when truncating virtual orbital subspace,[31–35] or the creation of an optimized virtual orbital subspace.[36–41] In the context of localized orbitals, specific correlation-capturing basis can be devised in order to limit the number of basis functions to some extent.[42]

In the present article, we show how two of these techniques, namely, approximating the remainder and optimizing the virtual orbitals, can be combined in order to obtain converged *GW* quasiparticle energies at a moderate computational cost for localized basis. We propose a definition of the reduced virtual orbital subspace that departs from the more conventional frozen natural orbital (FNO) technique,[36–39] because the FNO generation would quickly become computationally prohibitive for the largest systems. We would rather define the optimized virtual orbital subspace as the one spanned by a smaller localized basis. The remainder is then approximated by the one-ring self-energy (a simpler second order perturbation contribution to the self-energy), following the philosophy of the focal point analysis (FPA).[31,32] We demonstrate that the combination of both techniques is sufficient to obtain an estimate within 0.1 eV of the quasiparticle energies of molecules, even when calculating the *GW* self-energy in a simple double-ζ-polarized basis.

The article is organized as follows. We first quickly recap in Sec. II the key equations for the *GW* self-energy that will be necessary for the subsequent discussion. In Sec. III, we analyze the convergence rate of the different contributions to the *GW* self-energy and show how the one-ring self-energy can approximate the basis set dependence of the *GW* self-energy. In Sec. IV, we show how to build an optimized subspace from a single self-consistent field (SCF) calculation. The global performance of our approach is demonstrated in Sec. V, with an application to large graphene chunks.

II. *GW* SELF-ENERGY IN LOCALIZED BASIS

The *GW* approximation to the self-energy arises as the first order perturbation term, when the dynamically screened Coulomb interaction $W(\omega)$ is used as the perturbation parameter.[3,43] The dynamically screened Coulomb interaction is obtained within the so-called Random-Phase Approximation (RPA), which is synonym to the rings-only approximation to the screening. The Feynman representation of the *GW* self-energy is given in Fig. 1. As inferred from the diagrams, the *GW* self-energy is indeed an infinite summation over

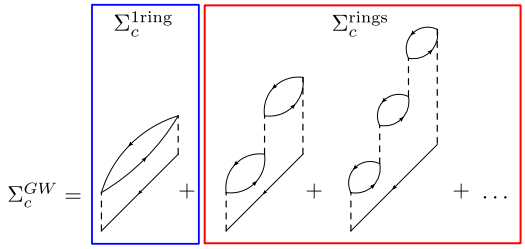

FIG. 1. Feynman diagrams for the correlation part of the *GW* self-energy Σ_c^{GW}. The arrows denote the Green's function G. The dashed line denotes the Coulomb interaction v. The *GW* self-energy is an infinite summation over the rings diagrams. It can be split into a sum of two terms: the one-ring self-energy $\Sigma_c^{1\text{ring}}$ and the several rings self-energy Σ_c^{rings}. The one-ring term is also named the direct term in the context of second-order perturbation theory.

the rings formed by two Green's functions in opposite directions. These rings account for the formation of electron-hole pairs.

The presentation of the *GW* self-energy is limited here to the crucial equations for conciseness. Many more details can be found, for instance, in Refs. 11, 12, 16, and 30. For simplicity, we limit our presentation here to spin-restricted calculations and to perturbative *GW*, where the self-energy is evaluated only once with self-consistent field (SCF) inputs.

Let us then specify directly the expectation value of the correlation part of the *GW* self-energy on the SCF eigenstate $|\varphi_p\rangle$,

$$\Sigma_{c\,pp}^{GW}(\omega) = 2\sum_{bs}\frac{(w_{pb}^s)^2}{\omega-\epsilon_b-\Omega_s+\mathrm{i}\eta} + 2\sum_{js}\frac{(w_{pj}^s)^2}{\omega-\epsilon_j+\Omega_s-\mathrm{i}\eta}, \quad (1)$$

where i, j run over occupied orbitals, a, b over virtual orbitals, and s over the neutral excitations. The small positive real number η ensures the correct positioning of the poles.

The coefficients w_{pi}^s and the energies Ω_s come from the spectral representation of $W(\omega) - v$,

$$(mn|W(\omega)-v|op) = \sum_s w_{mn}^s w_{op}^s \times\left(\frac{1}{\omega-\Omega_s+\mathrm{i}\eta}-\frac{1}{\omega+\Omega_s-\mathrm{i}\eta}\right), \quad (2)$$

where m, n, o, and p are indexes running over the eigenstates of the SCF Hamiltonian. We have introduced the difference $W - v$ in order to discard the exchange self-energy that poses no problem. We have chosen to present the *GW* formalism following the spectral function approach[30] for easiness. Of course, the conclusions drawn here are valid irrespective of the technical approach.

As shown in Fig. 1, the correlation part of the *GW* self-energy can naturally be decomposed into the one-ring contribution $\Sigma_c^{1\text{ring}}$ (termed the direct term in second-order perturbation theory) and the several-rings remainder Σ_c^{rings},

$$\Sigma_c^{GW} = \Sigma_c^{1\text{ring}} + \Sigma_c^{\text{rings}}. \quad (3)$$

Employing the Mulliken notation for the Coulomb integrals,

$$(pq|rs) = \int\int d\mathbf{r}d\mathbf{r}'\varphi_p(\mathbf{r})\varphi_q(\mathbf{r})\frac{1}{|\mathbf{r}-\mathbf{r}'|}\varphi_r(\mathbf{r}')\varphi_s(\mathbf{r}'), \quad (4)$$

the expression for $\Sigma_c^{1\text{ring}}$ can be obtained straightforwardly by considering that each neutral excitation s comes from a single transition from state i to state a. This approximation amounts to setting

$$\Omega_s = \epsilon_a - \epsilon_i \quad (5a)$$

$$w_{mn}^s = (mn|ia) \quad (5b)$$

in Eq. (2), which finally yields

$$\Sigma_{c\,pp}^{1\text{ring}}(\omega) = 2\sum_{bia}\frac{(pb|ia)^2}{\omega-\epsilon_b-\epsilon_a+\epsilon_i+\mathrm{i}\eta} + 2\sum_{jia}\frac{(pj|ia)^2}{\omega-\epsilon_j+\epsilon_a-\epsilon_i-\mathrm{i}\eta}. \quad (6)$$

At this stage, we have introduced the expressions for the *GW* self-energy and for the one-ring self-energy. In practice, the bottleneck in a *GW* calculation is most often the evaluation of $W(\omega)$. For instance, in the spectral decomposition approach,[14,16,33] this requires the diagonalization of the RPA matrix. This operation scales as N^6 since the RPA matrix has the dimension of the number of virtual orbitals times the number of occupied orbitals. Obviously, the calculation of $\Sigma_c^{1\text{ring}}$ skips this cumbersome step and is rather limited by the evaluation of the molecular orbital integrals in Eq. (4). This operation scales as N^5 in general or as N^4 if the Resolution-of-Identity approximation is used.[44] In Sec. III, we will evaluate how the information obtained for the simpler self-energy $\Sigma_c^{1\text{ring}}$ can be used to speed up the calculation of Σ_c^{GW}.

III. EXTRAPOLATION USING THE ONE-RING DIAGRAM

We propose to analyze in details how the different parts of the *GW* self-energy converge with respect to the calculation complexity. We exemplify here with the self-energy expectation value for the HOMO of benzene C_6H_6. The reference value is obtained with a very large Dunning-type basis,[45] the cc-pV6Z, that comprises 140 basis functions per carbon atom and 91 basis functions per hydrogen atom.

Two different strategies can be adopted to reduce the computational burden, as compared to the complete cc-pV6Z calculation: either one truncates the number of virtual orbitals used in the summations in Eqs. (1) and (2) or one employs a smaller basis. These two approaches are tested in Fig. 2, where the solid lines show the performance of the truncation of virtual orbitals in the cc-pV6Z basis, whereas the dashed lines illustrate the basis set convergence (cc-pV*n*Z). As the computational load is a function of the number of basis functions, it makes sense to compare the two strategies in terms of the accuracy reached for a given number of basis functions. With this criterium at hand, we conclude that the truncation strategy is far less efficient than the use of a smaller basis to minimize the error. In other words, though less flexible and then less accurate, the smaller basis set somehow better represents the virtual orbital subspace for a given number of basis functions.

The smaller basis induces a faster convergence for all the various parts of the self-energies we plotted in Fig. 2. From this

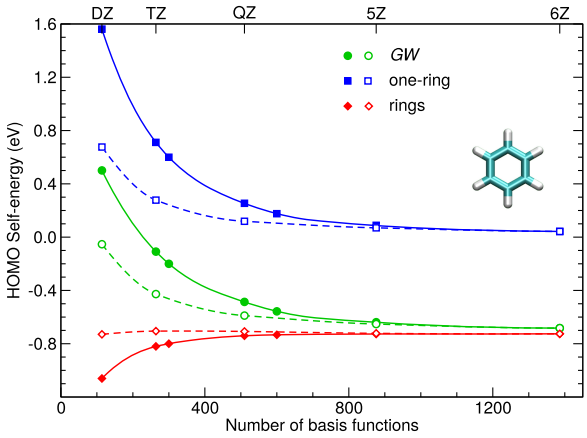

FIG. 2. Convergence of the self-energy contributions as a function of the number of states included in the self-energy for the HOMO of benzene. Two different convergence curves are shown: Solid lines are obtained from the most complete basis set (cc-pV6Z), however limiting the number of states included in the self-energy calculations; dashed lines are obtained by a standard basis set convergence study increasing the complexity n of the basis set (cc-pVnZ). The Dunning basis is labeled with a short-hand notation: DZ, TZ, etc.

observation, we conclude that it is a more sensible strategy to span the virtual orbital subspace with a small basis set, rather than with a large basis set however truncated at a given state index.

In Fig. 2, we decompose the *GW* self-energy following Eq. (3). It is clear that the slow convergence of the full *GW* self-energy Σ_c^{GW} mostly arises from the slow convergence of the one-ring term Σ_c^{1ring}. Indeed the difference between the latter two, Σ_c^{rings}, is already converged within 20 meV with the simplest basis cc-pVDZ.

The faster convergence of the higher-order terms was already observed in the context of coupled-cluster calculations.[31,32] The FPA strategy uses this property to perform accurate extrapolation to the complete basis set limit. It is used to extrapolate to the complete-basis set limit for high-level quantum chemistry methods,[21,46] assuming that the difference between higher-level methods (for instance, coupled-cluster) and lower-level methods (for instance, Møller-Plesset perturbation theory) converges quickly with the basis set complexity. Here we propose to adapt this strategy to the *GW* self-energy. Based on the observation of Fig. 2, we propose the following extrapolation formula:

$$\Sigma_{pp}^{GW\ \text{large}}(\omega) \approx \Sigma_{pp}^{GW\ \text{small}}(\omega) + \Sigma_{pp}^{\text{1ring large}}(\epsilon_p) - \Sigma_{pp}^{\text{1ring small}}(\epsilon_p), \quad (7)$$

where the basis set complexity (large or small) is specified in the superscript. Note that the *GW* self-energy is only evaluated within the small basis set. For numerical efficiency and also for accuracy, we have found advantageous to evaluate the one-ring contribution only at the SCF eigenvalue ϵ_p. The extrapolated self-energy curve is thus simply shifted as compared to the original loosely converged one.

In Sec. IV, we devise a practical scheme to evaluate the different terms of Eq. (7) with a single SCF calculation in the large basis. Though not absolutely necessary, this further step eases the application of the extrapolation formula for the user. Furthermore, this would circumvent issues that could arise if the state p used to bracket the self-energy changes too much from the small to the large basis sets.

IV. EVALUATION IN A SINGLE SCF CALCULATION

Our purpose here is to construct an optimized virtual orbital subspace based on a smaller basis out of an existing converged SCF calculation in a large basis. The development here is general to any basis set combination: The small basis does not need to be a subset of the larger one.

Let us label the basis functions of the large basis set $|\phi_A\rangle$ with a capitalized index A and the basis functions of the small basis set $|\phi_\alpha\rangle$ with a small greek letter α. The number of basis functions in the small basis is denoted by N_{small}, whereas the number of basis functions in the large basis is named N_{large}. At this stage, the converged SCF calculation provides us with the Hamiltonian matrix H_{AB}, its eigenvalues ϵ_p, and its eigenstate coefficents C_{Ap}, such that

$$|\varphi_p\rangle = \sum_{Ap} |\phi_A\rangle C_{Ap}. \quad (8)$$

Let us introduce the overlap matrix S,

$$S_{AB} = \langle\phi_A|\phi_B\rangle, \quad (9)$$

and the projection matrix S^{cross},

$$S_{A\alpha}^{\text{cross}} = \langle\phi_A|\phi_\alpha\rangle, \quad (10)$$

which connects the large basis to the small basis.

We define the effective basis functions $|\tilde{\phi}_\alpha\rangle$ that mimic the small basis functions however represented in the large basis as

$$|\tilde{\phi}_\alpha\rangle = \sum_{AB} |\phi_A\rangle S_{AB}^{-1} S_{B\alpha}^{\text{cross}}. \quad (11)$$

Now, one can work in the subspace spanned by the N_{small} basis functions defined in Eq. (11). The corresponding Hamiltonian $\tilde{H}$ and overlap matrix $\tilde{S}$ read

$$\tilde{H}_{\alpha\beta} = \sum_{ABCD} S_{A\alpha}^{\text{cross}} S_{AB}^{-1} H_{BC} S_{CD}^{-1} S_{D\beta}^{\text{cross}}, \quad (12a)$$

$$\tilde{S}_{\alpha\beta} = \sum_{AB} S_{A\alpha}^{\text{cross}} S_{AB}^{-1} S_{B\beta}^{\text{cross}}, \quad (12b)$$

where the symmetry of the S^{-1} matrix was used to simplify the expression.

Hence, the Roothaan-Hall equation can be solved in the small subspace,

$$\tilde{H}\tilde{C} = \tilde{S}\tilde{C}\tilde{E}, \quad (13)$$

to obtain the eigenvalues $\tilde{E}$ and eigenvectors $\tilde{C}$. The eigenvectors coefficients can be then brought back to the original large basis (capitalized indexes), with the transform

$$\tilde{C}'_{Ap} = \sum_{B\alpha} S_{AB}^{-1} S_{B\alpha}^{\text{cross}} \tilde{C}_{\alpha p}. \quad (14)$$

Instead of using directly the new coefficients $\tilde{C}'_{Ap}$ for all states p, one would like to circumvent a potential issue. Since the smaller basis may not contain the same basis functions as the larger one, the bracketing state p used to obtain the expectation value of the self-energy may change when shifting from the large basis to the small effective basis. To prevent this, we

choose to freeze the occupied states together with the bracketing states into their original expression. This procedure is completely analogous to the one used in frozen natural orbital technique, except that here the frozen orbitals may comprise the few first virtual orbitals used to evaluate the self-energy expectation value.

The different subspaces we defined are depicted in Fig. 3 in the prototypical case where the self-energy is evaluated for the HOMO and LUMO. The N_f orbitals up to the LUMO will be kept frozen to their expression in the large basis set. The virtual orbitals indexed from $N_f + 1$ to the size of the small basis N_{small} will be optimized and finally, the virtual orbitals above N_{small} will be simply discarded from the *GW* calculation. The precise index N_f can be slightly increased in order to avoid splitting degenerate orbitals into different subspaces.

The described scheme can be written down as an update of the $\tilde{C}'$ coefficients,

$$\tilde{C}'_{Ap} \leftarrow \begin{cases} C_{Ap} & \text{for} \quad p \le N_f \\ \tilde{C}'_{Ap} & \text{for} \quad N_f < p \le N_{\text{small}} \\ 0 & \text{for} \quad N_{\text{small}} < p \le N_{\text{large}}. \end{cases} \tag{15}$$

Then the Roothaan-Hall equations are solved once again in the new subspace spanned by the N_{small} orbitals, whose coefficients are the new $\tilde{C}'_{Ap}$,

$$\bar{H} = \tilde{C}'^T H \tilde{C}', \tag{16a}$$

$$\bar{S} = \tilde{C}'^T S \tilde{C}', \tag{16b}$$

$$\bar{H}\bar{C} = \bar{S}\bar{C}\bar{E}. \tag{16c}$$

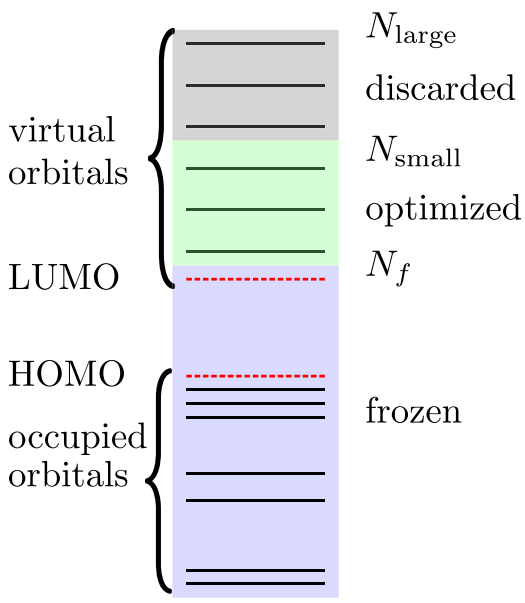

FIG. 3. Diagrammatic representation of the various orbital subspaces. Electronic states are the horizontal lines. As a typical example, we choose to evaluate the *GW* self-energy for the HOMO and the LUMO, shown with dashed red lines. The blue area designates the frozen subspace, which encompasses the occupied states and the ones used to bracket the self-energy. The green area shows the optimized subspace identified through a smaller basis set. The gray area identifies the electronic states that will be discarded from the *GW* self-energy calculation.

and the final coefficients read

$$C_{Ap} \leftarrow \begin{cases} \sum_q \tilde{C}'_{Aq} \bar{C}_{qp} & \text{for} \quad p \le N_{\text{small}} \\ 0 & \text{for} \quad N_{\text{small}} < p \le N_{\text{large}}, \end{cases} \tag{17}$$

and the final energies are

$$\epsilon_p \leftarrow \begin{cases} \bar{\epsilon}_p & \text{for} \quad p \le N_{\text{small}} \\ 0 & \text{for} \quad N_{\text{small}} < p \le N_{\text{large}}. \end{cases} \tag{18}$$

By construction of the $\tilde{C}'$ basis, the N_f first eigenvectors and eigenvalues obtained in Eqs. (17) and (18) remain identical to the original ones.

With this construction of the reduced virtual subspace, we can proceed with the practical evaluation of the performance of the scheme.

V. A FEW APPLICATIONS

The calculations presented here are standard one-shot *GW* calculations based on hybrid functional SCF inputs, obtained from PBE0[47] (*GW*@PBE0) or from BHLYP[48] (*GW*@BHLYP). We use the Resolution-of-Identity approximation to avoid the 4-center Coulomb integrals. We concentrate on Dunning-type basis sets,[45] since they offer the possibility of systematic improvement. Note that this basis set family is not nested, meaning that the triple-ζ basis does not necessarily contain the basis functions of the double-ζ basis.

We have implemented the optimization of the virtual subspace described in Eqs. (17) and (18) in the *GW* code named MOLGW.[30,49] The spectral method implemented in MOLGW requires the diagonalization of the RPA matrix in the product basis. As the product basis grows as N^2 for N atoms, this operation scales as N^6 and is the actual bottleneck of the method. In this context, it is crucial to keep the dimension of the product basis as small as possible. This subspace definition is used to evaluate the extrapolation formula of Eq. (7) in a single run. MOLGW first performs the SCF calculations, followed by the *GW* and the one-ring calculations in the reduced subspace, and finally the one-ring evaluation in the complete basis set.

Let us first come back to the benzene example we already used in Sec. III. Figure 4 shows the convergence of the *GW*@PBE0 HOMO quasiparticle energy as a function of the basis set used in the *GW* calculation. The standard approach in which the basis set is kept the same in the prior SCF step and in the *GW* post-processing (green dashed line) experiences the usual dramatically slow convergence.

Then, we trigger the optimized subspace generation and the extrapolation formula. Following the results obtained with the largest basis set for the SCF step (cc-pV6Z, red line with down triangles), we can appreciate how fast the convergence with respect to the basis set in the *GW* part becomes. The error with the simplest basis (cc-pVDZ) is only 20 meV and goes down to less than 10 meV for the next rung (cc-pVTZ).

Following a vertical black line in Fig. 4, one can appreciate how the convergence behavior is captured by simple calculations in which the basis set in the *GW* part is kept fixed and only the SCF basis is increased.

The same type of convergence plot is provided in the more complex case of a noble metal cluster in Fig. 5. There, we

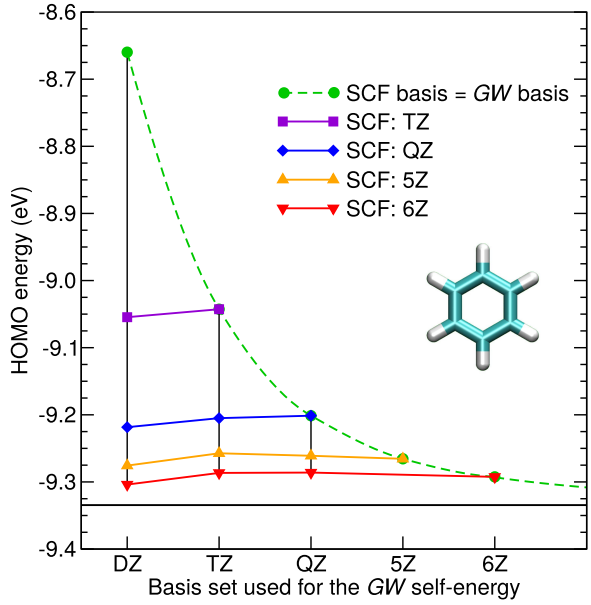

FIG. 4. Convergence plot of the HOMO of benzene within *GW*@PBE0 as a function of the basis set used in the *GW* self-energy. The green dashed line shows a regular convergence plot when the basis set for SCF and *GW* is the same. The horizontal black line is the extrapolated HOMO in the complete basis set limit. The violet, blue, orange, and red symbols encode the SCF basis set.

consider an 8-atom silver cluster, whose atomic coordinates were obtained from Ref. 50. This system is very different from the previous case of benzene: it has a relatively small HOMO-LUMO gap and it contains highly localized 4*d* electrons. First of all, the convergence of the 4*d* states by brute force increase of the basis set complexity (green dashed line) is much slower than the 5*s* HOMO state. The optimized subspace plus extrapolation technique we propose works extremely well for the 4*d* state. The correction for the 5*s* state has a tendency

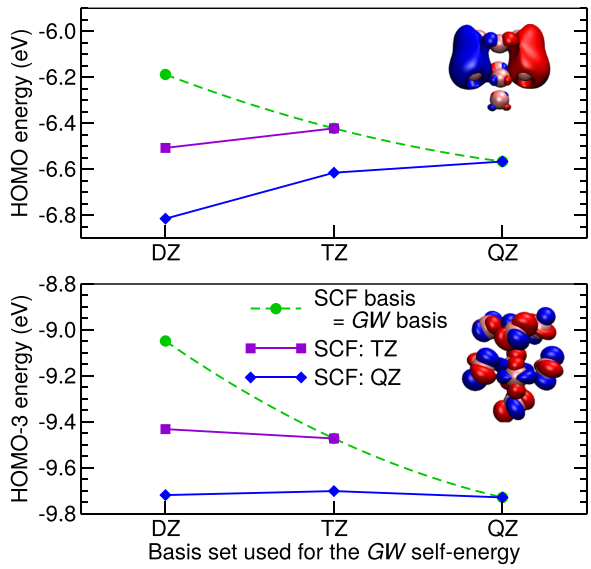

FIG. 5. Convergence plot of the HOMO (with *s* character, upper panel) and the HOMO-3 (with *d* character, lower panel) of a silver cluster Ag_8 within *GW*@PBE0 as a function of the basis set used in the *GW* self-energy. The green dashed line shows a regular convergence plot when the basis set for SCF and *GW* is the same. The violet and blue symbols encode the SCF basis set.

to overshoot; however, using the cc-pVTZ basis to span the virtual subspace of the *GW* is already enough to reduce it.

Beyond the case of benzene and of the Ag_8 cluster, we applied the same procedure to the HOMO quasiparticle energy of the 34-small-molecule set introduced in Ref. 10. Figure 6 shows the mean signed error of the HOMO energy within *GW*@PBE0, with respect to the reference taken as the cc-pV5Z results. This benchmark is more stringent for the extrapolation scheme, as we observe that the proposed approach generally performs better for larger molecules. Evaluating the self-energy within the cc-pVDZ basis set yields an average error of about 0.1 eV that might be considered as slightly too large for the typical requested accuracy. However, using the subsequent basis set, cc-pVTZ, cuts the average error down to 0.06 eV. The convergence rate is anyway much faster than the standard procedure shown with the dashed green line.

We now demonstrate the potentiality of the proposed technique with the calculation the HOMO and LUMO quasiparticle energies of very large graphene chunks[51] within *GW*@BHLYP. Here we selected the BHLYP SCF starting point, since it usually induces a nice agreement with respect to experiment.[17,52] The carbon-carbon bond length is set to 1.42 Å and the hydrogen-carbon one to 1.09 Å.

The results reported in Fig. 7 have been obtained with the cc-pVQZ quality, by using the cc-pVQZ for the SCF step and the extrapolation formula with a cc-VDZ optimized virtual orbital subspace. With the largest system, $C_{150}H_{30}$, containing as many as 180 atoms and comprising as many as 9150 basis functions, the SCF calculation can already be considered as challenging. The *GW* calculation is then performed using the optimized basis set with 2250 basis functions instead.

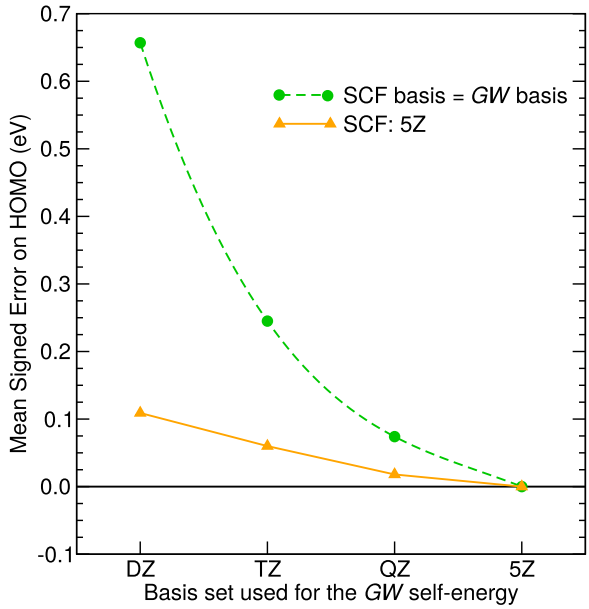

FIG. 6. Mean signed error of the *GW*@PBE0 HOMO energies of a 34 molecule set as a function of the basis set used in the *GW* self-energy. The green dashed line shows a regular convergence plot when the basis set for SCF and *GW* is the same. The horizontal black line is the reference set for the cc-pV5Z basis. The orange triangle symbols show the convergence with a fixed SCF basis set, namely, cc-pV5Z.

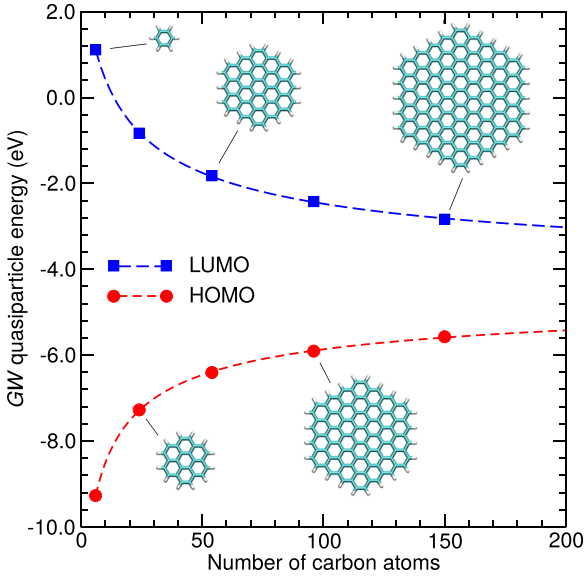

FIG. 7. Evolution of HOMO and LUMO quasiparticle energies within *GW*@BHLYP as a function of the number of carbon atoms in graphene chunks, C_6H_6, $C_{24}H_{12}$, $C_{54}H_{18}$, $C_{96}H_{24}$, and $C_{150}H_{30}$. The SCF basis set is cc-pVQZ, whereas the *GW* self-energy was evaluated for a cc-pVDZ-based virtual subspace.

As shown in Fig. 7, the HOMO and LUMO quasiparticle energies can be nicely fit with a linear function on $n^{-1/2}$, where n is the number of carbon atoms in the system. From these fits, the work function of an infinite graphene sheet work function is extrapolated to 4.35 eV. Note that the BHLYP extrapolated value is noticeably lower, 3.95 eV.

VI. CONCLUSION

In this article, we have demonstrated the possibility to accelerate the slow convergence of the *GW* self-energy through the combination of two techniques: first, we create an reduced virtual orbital subspace as spanned by a smaller basis set; second, we evaluate the error between the complete subspace and the reduced one, thanks to the simpler one-ring self-energy Σ_c^{1ring}. These two steps do not affect the overall comptutational scaling of a *GW* calculation; however, the prefactor is drastically reduced.

The accuracy of this method has been assessed on small molecules, for which large basis reference calculations were achievable. We have further shown the possibility to calculate very large molecules using what is generally considered as a very good basis set (cc-pVQZ). To the best of our knowledge, our *GW* calculation of the HOMO/LUMO quasiparticle energy of $C_{150}H_{30}$ is one of the most massive *GW* calculations published in the literature to date.

We emphasize that the proposed scheme is extremely simple for the end user. The computer code is run only once and the only input requested from the user is the choice of the smaller basis employed to span the reduced virtual subspace.

The present developments will certainly broaden the range of applications for the *GW* self-energy for molecular systems and clusters. These advances are available in the development version of MOLGW.[49]

ACKNOWLEDGMENTS

This work was performed using HPC resources from GENCI-CCRT-TGCC (Grant No. 2016-096018).

[1] A. L. Fetter and J. D. Walecka, *Quantum Theory of Many-Particle Systems* (MacGraw-Hill, New York, 1971).
[2] A. Szabó and N. S. Ostlund, *Modern Quantum Chemistry: Introduction to Advanced Electronic Structure Theory* (Dover Publications, Mineola, NY, 1996).
[3] L. Hedin, Phys. Rev. **139**, A796 (1965).
[4] M. S. Hybertsen and S. G. Louie, Phys. Rev. B **34**, 5390 (1986).
[5] R. W. Godby, M. Schlüter, and L. J. Sham, Phys. Rev. B **37**, 10159 (1988).
[6] G. Onida, L. Reining, and A. Rubio, Rev. Mod. Phys. **74**, 601 (2002).
[7] M. Rohlfing, Int. J. Quantum Chem. **80**, 807 (2000).
[8] J. C. Grossman, M. Rohlfing, L. Mitas, S. G. Louie, and M. L. Cohen, Phys. Rev. Lett. **86**, 472 (2001).
[9] M. L. Tiago, J. C. Idrobo, S. Öğüt, J. Jellinek, and J. R. Chelikowsky, Phys. Rev. B **79**, 155419 (2009).
[10] C. Rostgaard, K. W. Jacobsen, and K. S. Thygesen, Phys. Rev. B **81**, 085103 (2010).
[11] X. Blase, C. Attaccalite, and V. Olevano, Phys. Rev. B **83**, 115103 (2011).
[12] X. Ren, P. Rinke, V. Blum, J. Wieferink, A. Tkatchenko, A. Sanfilippo, K. Reuter, and M. Scheffler, New J. Phys. **14**, 053020 (2012).
[13] N. Marom, F. Caruso, X. Ren, O. T. Hofmann, T. Körzdörfer, J. R. Chelikowsky, A. Rubio, M. Scheffler, and P. Rinke, Phys. Rev. B **86**, 245127 (2012).
[14] F. Bruneval, J. Chem. Phys. **136**, 194107 (2012).
[15] S. Sharifzadeh, I. Tamblyn, P. Doak, P. Darancet, and J. Neaton, Eur. Phys. J. B **85**, 323 (2012).
[16] M. J. van Setten, F. Weigend, and F. Evers, J. Chem. Theory Comput. **9**, 232 (2013).
[17] F. Bruneval and M. A. L. Marques, J. Chem. Theory Comput. **9**, 324 (2013).
[18] S. Körbel, P. Boulanger, I. Duchemin, X. Blase, M. A. L. Marques, and S. Botti, J. Chem. Theory Comput. **10**, 3934 (2014).
[19] M. Govoni and G. Galli, J. Chem. Theory Comput. **11**, 2680 (2015).
[20] M. J. van Setten, F. Caruso, S. Sharifzadeh, X. Ren, M. Scheffler, F. Liu, J. Lischner, L. Lin, J. R. Deslippe, S. G. Louie, C. Yang, F. Weigend, J. B. Neaton, F. Evers, and P. Rinke, J. Chem. Theory Comput. **11**, 5665 (2015).
[21] T. Rangel, S. M. Hamed, F. Bruneval, and J. B. Neaton, J. Chem. Theory Comput. **12**, 2834 (2016).
[22] X. Blase, P. Boulanger, F. Bruneval, M. Fernandez-Serra, and I. Duchemin, J. Chem. Phys. **144**, 034109 (2016).
[23] C. Møller and M. S. Plesset, Phys. Rev. **46**, 618 (1934).
[24] R. J. Bartlett and M. Musiał, Rev. Mod. Phys. **79**, 291 (2007).
[25] B.-C. Shih, Y. Xue, P. Zhang, M. L. Cohen, and S. G. Louie, Phys. Rev. Lett. **105**, 146401 (2010).
[26] M. Stankovski, G. Antonius, D. Waroquiers, A. Miglio, H. Dixit, K. Sankaran, M. Giantomassi, X. Gonze, M. Côté, and G.-M. Rignanese, Phys. Rev. B **84**, 241201 (2011).
[27] C. Schwartz, in *Methods in Computational Physics*, edited by B. J. Alder (Academic Press, New York, 1963), Vol. 2.
[28] P. Umari, G. Stenuit, and S. Baroni, Phys. Rev. B **81**, 115104 (2010).
[29] J. Klimeš, M. Kaltak, and G. Kresse, Phys. Rev. B **90**, 075125 (2014).
[30] F. Bruneval, T. Rangel, S. M. Hamed, M. Shao, C. Yang, and J. B. Neaton, Comput. Phys. Commun. **208**, 149 (2016).
[31] A. L. L. East and W. D. Allen, J. Chem. Phys. **99**, 4638 (1993).
[32] A. G. Császár, W. D. Allen, and H. F. Schaefer, J. Chem. Phys. **108**, 9751 (1998).
[33] M. L. Tiago and J. R. Chelikowsky, Phys. Rev. B **73**, 205334 (2006).
[34] F. Bruneval and X. Gonze, Phys. Rev. B **78**, 085125 (2008).
[35] J. Deslippe, G. Samsonidze, M. Jain, M. L. Cohen, and S. G. Louie, Phys. Rev. B **87**, 165124 (2013).
[36] C. Sosa, J. Geertsen, G. W. Trucks, R. J. Bartlett, and J. A. Franz, Chem. Phys. Lett. **159**, 148 (1989).
[37] D. Feller, J. Chem. Phys. **98**, 7059 (1993).
[38] A. G. Taube and R. J. Bartlett, J. Chem. Phys. **128**, 164101 (2008).
[39] F. Aquilante, T. K. Todorova, L. Gagliardi, T. B. Pedersen, and B. O. Roos, J. Chem. Phys. **131**, 034113 (2009).
[40] F. Neese, A. Hansen, and D. G. Liakos, J. Chem. Phys. **131**, 064103 (2009).
[41] C. Riplinger and F. Neese, J. Chem. Phys. **138**, 034106 (2013).
[42] I. Y. Zhang, X. Ren, P. Rinke, V. Blum, and M. Scheffler, New J. Phys. **15**, 123033 (2013).

[43]F. Aryasetiawan and O. Gunnarsson, Rep. Prog. Phys. **61**, 237 (1998).
[44]F. Weigend, M. Häser, H. Patzelt, and R. Ahlrichs, Chem. Phys. Lett. **294**, 143 (1998).
[45]T. H. Dunning, J. Chem. Phys. **90**, 1007 (1989).
[46]M. S. Deleuze, L. Claes, E. S. Kryachko, and J.-P. Franois, J. Chem. Phys. **119**, 3106 (2003).
[47]C. Adamo and V. Barone, J. Chem. Phys. **110**, 6158 (1999).
[48]A. D. Becke, J. Chem. Phys. **98**, 1372 (1993).
[49]See http://www.molgw.org for download, manual, and examples.
[50]E. M. Fernández, J. M. Soler, I. L. Garzón, and L. C. Balbás, Phys. Rev. B **70**, 165403 (2004).
[51]D. L. Strout and G. E. Scuseria, J. Chem. Phys. **102**, 8448 (1995).
[52]F. Bruneval, S. M. Hamed, and J. B. Neaton, J. Chem. Phys. **142**, 244101 (2015).